EVOLUTION & ECOLOGY

Correspondence and requests for materials should be addressed to DE (email: devangel77b@gmail.com).

Shifts in stability and control effectiveness during evolution of the Avialae support aerial manoeuvring hypotheses for flight origins

Dennis Evangelista[1,5], Sharlene Cam[1], Tony Huynh[1], Austin Kwong[2], Homayun Mehrabani[2], Kyle Tse[3] & Robert Dudley[1,4]

[1]Department of Integrative Biology, University of California, Berkeley; [2]Department of Bioengineering, University of California, Berkeley; [3]Department of Mechanical Engineering, University of California, Berkeley; [4]Smithsonian Tropical Research Institute, Balboa, Panama; [5]current address Department of Biology, University of North Carolina at Chapel Hill, NC

The capacity for aerial manoeuvring shaped the evolution of flying animals. Here we evaluate consequences of aviaian morphology for aerial performance[1,2] by quantifying static stability and control effectiveness of physical models[3] for numerous taxa sampled from within the lineage leading to birds (Avialae[4]). Results of aerodynamic testing are mapped phylogenetically[5-9] to examine how manoeuvring characteristics correlate with tail shortening, fore- and hindwing elaboration, and other morphological features[10]. In the evolution of the Avialae we observe shifts from static stability to inherently unstable aerial planforms; control effectiveness also migrated from tails to the forewings. These shifts suggest that some degree of aerodynamic control and and capacity for manoeuvring preceded the evolution of strong power stroke. The timing of shifts suggests features normally considered in light of development of a power stroke also play important roles in control.

Regardless of how aerial behaviour originates, once airborne an organism must control[2] its orientation and position in order to safely navigate the vertical environment (i.e. gliding and directed aerial descent[1]). Such abilities are present even in taxa with no obvious morphological adaptation for flight; at low speeds, such as at the start of a fall or jump, inertial mechanisms allow for rolling, pitching, and yawing; as speeds increase (or as appendages grow in area), aerodynamic mechanisms of control can be employed. Body and appendage configuration position affect both stability, the tendency to resist perturbations, as well as production of torques and forces for manoeuvring (control effectiveness). In the four-winged mid-Cretaceous *Microraptor gui*, changes in planform, such as alternative reconstruction postures or removal of leg and tail feathers, alter stability and the control effectiveness of appendages[3]. Furthermore, appendage function can shift entirely according to the aerial environment (e.g. asymmetric wing pronation producing yaw at high glide angle versus roll at low glide angle) or

even completely reverse function[3]. Such results are exciting but are based on a single specimen[11]. Stronger conclusions can be drawn from comparative study of several forms within a phylogenetic context.

One obvious trend in avian evolution is the transition from long tails and feathered legs in early forms[11–14] to later (including extant) forms for which the tail has fused into a short pygostyle and asymmetric flight feathers are absent from the legs. Functional consequences of this shift remain speculative[15–17]. Similarly, changes in the pectoral girdle have been assumed to enhance a powered downstroke[4,10], but may also have influenced manoeuvring by shifting the centre of body mass[18] or in enabling the production of wing asymmetries.

To examine these patterns and to cross-test adaptive hypotheses[19], we can use model tests to quantify the effect of shape on stability and control effectiveness[3], using specimens sampled from early avialan[4] evolution[6–8]. We hypothesize that within the Avialae, the presence or absence of stability in the various axes and the control effectiveness of the appendages should correlate with changes in major morphological features (shortening of the tail, enlargement of the forewings) to enhance aerodynamic performance. Alternatively, both stability and control may have been absent early in the evolution of flight, only appearing after a strong and bilaterally symmetric power stroke evolved.

Representative aerodynamic measurements for pitching stability and control effectiveness are given in Fig. 1 for seven avialans. Tables and plots of all aerodynamic measurements are provided in the Supplemental Information. Long-tailed taxa (Fig. 1.a) show a stable equilibrium point and the tail is effective in generating pitching moments, whereas short-tailed taxa (Fig. 1.b) were unstable and had reduced control effectiveness of the tail. Notably, the same pattern (i.e., downward sloping C_m versus α) is seen consistently in two early representatives of the Avialaes, in a long-tailed pterosaur (*Rhamphorynchus*), and in the mid-Cretaceous dromaeosaur *Microraptor*, suggesting that these patterns more likely derive from shape and aerodynamics than from immediate ancestry.

All aerodynamic measurements were coded into both discretized and continuous character matrices (see Supplemental Information), which were then mapped onto the phylogeny to examine the evolution of static stability and control effectiveness.

The Avialae show progressive tail loss as well as loss of leg-associated control surfaces along with a concomitant increase in forewing size and bony features associated with the pectoral girdle (nodes 1-4 on Fig. 2). Changes in stability and control effectiveness reflect these morphological changes. In pitch (Fig. 2), taxa shift from being statically stable ancestrally to subsequently being unstable (and thus requiring active control). Control effectiveness concomitantly migrates from the ancestrally large and feathered tail and legs to the increasingly capable forewings, which become relatively larger, gain larger muscle attachments and gain skeletal features that improve production of fine left-right and fore-aft kinematic asymmetries needed for control.

Transition to forewing control correlates with elongation of the coracoid, along with other changes in the scapula (Fig. 2, node 2); in addition, the sternum becomes modified (although a strong keel has not yet developed)[10]. Concomitantly, the tail becomes much reduced into a pygostyle (Fig. 2, node 3). Other synapomorphies (Fig. 2, node 4) appear in the mid-Cretaceous, including the strut-like coracoid, triosseal canal, synsacrum and carinate sternum. Whereas the latter features (node 4) feature in power production, the timing of the former features (nodes 2 and 3) appears consistent with enhanced forewing control effectiveness. Ontogenetic tests[20] show 4-day post hatching chukar are capable of extreme manoeuvres (rolling and pitching 180°) before strong development of a carinate sternum, suggesting this interpretation is correct.

In roll (Fig. 3), taxa were stable at high angles of attack, but either unstable or marginally stable at low angles of attack; large asymmetric wing movements (i.e., wing tucking) was always effective in creating substantial rolling moments.

In yaw, all taxa at high angles of attack (Fig. 4a) were marginally stable as might be expected from symmetry. Taxa with long tails were also stable at low angle-of-attack (Fig. 4b) but as tails are reduced, yaw stability is lost and control must again migrate

to the wings. Asymmetric wing pronation and supination (Fig. 4a and 4b) was effective in generating yawing moments in all taxa, suggesting manoeuvrability in yaw early in bird evolution. As the tail becomes shorter, flight becomes marginally stable or unstable, and control effectiveness must migrate (as in pitch control) from the shortening tail to the enlarging forewings. Stability in roll and in yaw shifts with angle of attack, which may serve as a proxy for glide angle or the steepness of descent. At high angles of attack, roll is the more stable axis, whereas stability in yaw is greater at low angles of attack. Forewing asymmetrical movements were effective in all taxa, whereas forewing symmetrical movements were only effective in later taxa.

The findings suggest that the capacity for manoeuvring characterized the early stages of flight evolution[1], before forewings with a power stroke fully evolved. The large tail of early Avialaes yielded high aerodynamic control effectiveness and the body possessed some degree of stability. Combined with likely dynamic forces and torques generated by either tail whipping[21] or reduced amounts of asymmetric or symmetric forewing flapping, this suggests that the ancestral organisms were very capable of controlled aerial behaviours at high angles of attack (Figs. 2-4). Subsequent shifts in control would be consistent with more shallow glides facilitated by incipient wing flapping, which may have served initially in control but then ultimately became the power stroke characteristic of modern birds. Incipient flapping may thus have become elaborated as a control response[2] to instabilities demonstrated here. Active control was required as static stability was reduced and eventually lost, and associated forewing movements would also have enhanced aerodynamic force production and provided a means for inertial attitude adjustment. Once the transition to wing-mediated manoeuvrability and control began, larger surfaces and increased musculature would have facilitated dynamic force production for weight offset via the power stroke characteristic of modern birds.

Methods

We constructed models (8 cm snout-vent length) of four extant birds, six avialans[4] plus *Microraptor*[11] and *Anchiornis*[12] as outgroups, using 3D printing[22] (extended Figs. 5 and 6). Fossils were selected to sample available phylogenies. To explore parallel

evolution and for calibration, we also constructed models of three pterosaurs, two bats, and two artificial test objects (sphere and weather vane). Theropods were reconstructed with wings spread and legs extended back[3,23] (extended Figs. 6 and 7). For control effectiveness, we tested appendage movements previously identified as being aerodynamically effective[3,20]: asymmetric wing pronation and supination, wing tucking, symmetric wing protraction and retraction, and dorsoventral and lateral movements of the tail (extended Fig. 7).

Wind tunnel testing used established methods[3], with a six-axis sensor (Nano17, ATI, Apex, NC) mounted to a 0.5 inch (12.7 mm) damped sting exiting the model downwind at the centre of mass (extended Fig. 6). Testing at 6 ms^{-1} resulted in a Reynolds number of ~32,000 for all models, matching full scale for *Archaeopteryx*. Under these conditions the aerodynamic coefficients of interest are reasonably constant with Re[3,20].

Sensor readings were recorded at 1000 Hz using a data acquisition card (National Instruments, Austin, TX)[3]. The sting was mounted to a servo (Hitec USA, Poway, CA) interfaced to a data acquisition computer, using an Arduino microcontroller (SparkFun, Boulder, CO) and specially written code in Python and R[24], to automate positioning and measurement of windspeed and force/torque. We then computed non-dimensional force and moment coefficients, static stability coefficients, and control effectiveness[3,25]. Using the automatic sting, we obtained 13,792 measurements for 247 positions (86 in pitch, 69 in roll, and 92 in yaw).

A Nexus file without branch lengths was assembled from published phylogenies[6–9] of the study taxa. Mapping of discrete manoeuvring traits was performed in Mesquite[5] with the built-in ancestral state reconstruction routines using unordered parsimony. Aerodynamic measurements were coded into a matrix giving eight discretised stability values (stable, marginal, unstable); ten discrete morphological traits, and 12 discretised control effectiveness values (using a threshold of 0.09, chosen based on the weather vane measurements). Additional information is provided in the Supplementary Methods.

1. Dudley, R. & Yanoviak, S. P. Animal aloft: the origins of aerial behavior and flight. *Integr. Comp. Biol.* **51,** 926–936 (2011).
2. Smith, J. M. The importance of the nervous system in the evolution of animal flight. *Evolution* **6,** 127–129 (1952).
3. Evangelista, D. *et al.* Aerodynamic characteristics of a feathered dinosaur measured using physical models . Effects of form on static stability and control effectiveness. *PLoS ONE* (2014). doi:10.1371/journal.pone.0085203
4. Gauthier, J. & Padian, K. in *Beginnings of the Birds: Proceedings of the International Archaeopteryx Conference* (Hecht, M. K., Ostrom, J. H., Viohl, G. & Wellnhover, P.) 185–197 (Freunde des Jura-Museums, 1985).
5. Maddison, W. P. & Maddison, D. R. Mesquite: A modular system for evolutonary analysis. (2010). http://mesquiteproject.org
6. Zhou, ZH. & Li, F. Z. Z. A new Lower Cretaceous bird from China and tooth reduction in early avian evolution. *Proc. R. Soc. B.* **277,** 219–227 (2010).
7. Li, Q. *et al.* Plumage color patterns of an extinct dinosaur. *Science.* **327,** 1369–1372 (2010).
8. O'Connor, J., Chiappe, L. M. & Bell, A. in *Living Dinosaur: Evolutionary History of the Modern Birds* (Dyke, G. & Kaiser, G.) 39–105 (John Wiley & Sons, 2011).
9. Cracraft, J. *et al.* in *Assembling the Tree of Life* (Cracraft, J. & Donoghue, M. J.) 468–489 (Oxford University Press, 2004).
10. Benton, M. J. *Vertebrate Paleontology.* (Blackwell Publishing, 2005).
11. Xu, X. *et al.* Four-winged dinosaurs from China. *Nature* **421,** 335-340 (2003).
12. Hu, D., Hou, L., Zhang, L. & Xu, X. A pre-*Archaeopteryx* troodontid theropod from China with long feathers on the metatarsus. *Nature* **461,** 640–643 (2009).
13. Longrich, N. Structure and function of hindlimb feathers in *Archaeopteryx* lithographica. *Paleobiology* **32,** 417–431 (2006).
14. Christiansen, P. & Bonde, N. Body plumage in *Archaeopteryx*: a review, and new evidence from the Berlin specimen. *Comptes Rendus Palevol* **3,** 99–118 (2004).
15. Smith, J. M. Birds as aeroplanes. *New Biol.* **14,** 64–81 (1953).
16. Beebe, C. W. A tetrapteryx stage in the ancestry of birds. *Zoologica* **2,** 39–52 (1915).
17. Thomas, A. L. R. On the tails of birds. *Bioscience* **47,** 215–225 (1997).
18. Allen, V., Bates, K. T., Li, Z. & Hutchinson, J. R. Linking the evolution of body shape and locomotor biomechanics in bird-line archosaurs. *Nature* **497,** 104–107 (2013).
19. Padian, K. Cross-testing adaptive hypotheses: Phylogenetic analysis and the origin of bird flight. *Amer. Zool.* **41,** 598–607 (2001).
20. Evangelista, D. J. Aerial Righting, Directed Aerial Descent, and Maneuvering in the Evolution of Flight in Birds. Ph.D. thesis, U.C. Berkeley (2013).
21. Jusufi, A., Goldman, D. I., Revzen, S. & Full, R. J. Active tails enhance arboreal acrobatics in geckos. *Proc Nat Acad Sci USA* **105,** 4215–4219 (2008).
22. Munk, J. D. The Descent of Ant. Ph.D. thesis, U.C. Berkeley (2011).
23. Xu, X., Zhou, ZH., Zhang, FC., Wang, XL. & Kuang, XW. Functional hind-wings conform to the hip structure in dromaeosaurids. *J. Vert. Palaeo.* **24**:251 (2004).

24. R Core Team. R: A Language and Environment for Statistical Computing. (2013). http://www.r-project.org/
25. McCormick, B. W. *Aerodynamics, Aeronautics and Flight Mechanics*. (John Wiley and Sons, 1995).
26. Zhou, ZH. & Zhang, FC. A long-tailed seed-eating bird from the Early Cretaceous of China. *Nature* **418**, 405-409 (2002).
27. Zhou, ZH. & Zhang, FC. *Jeholornis* compared to *Archaeopteryx*, with a new understanding of the earliest avian evolution. *Naturwissenschaften* **90**:220-225 (2003).
28. Gao, CL. *et al.* A new basal lineage of early Cretaceous birds from China and its implications on the evolution of the avian tail. *Palaeontology* **51**, 775-791 (2008).
29. Zhou, ZH. & Zhang, FC. Anatomy of the primitive bird *Sapeornis chaoyangensis* from the early Cretaceous of Liaoning, China. *Can J. Earth Sci.* **40**, 731-747 (2003).
30. Hou, LH., Zhou, ZH., Martin, L. & Feduccia, A. A beaked bird from the Jurassic of China. *Nature* **377**, 616-618 (1995).

Supplementary Information is available in the online version of the paper.

Acknowledgements We thank Y Munk, Y Zeng, E Kim, M Wolf, N Sapir, V Ortega, S Werning, K Peterson, J McGuire and R Fearing for their advice and assistance. We than the Berkeley Undergraduate Research Apprentice Program (URAP) and the help of G Cardona, C Chun, M Cohen, E Guenther-Gleason, V Howard, S Jaini, F Linn, C Lopez, A Lowenstein, D Manohara, D Marks, N Ray, A Tisbe, F Wong, O Yu and R Zhu. DE was supported by an NSF Minority Graduate Research Fellowship, UC Chancellor's Fellowship, and NSF Integrative Graduate Education and Research Traineeship (IGERT) #DGE-0903711. TH was supported by the University of California Museum of Palaeontology (UCMP). We also thank T Libby and the Berkeley Centre for Integrative Biomechanics in Education and Research (CIBER) for use of a force sensor and 3D printer.

Author Contributions DE wrote the main manuscript text with assistance from RD and TH; DE and TH prepared figures; all authors contributed to the manuscript. The authors declare that they have no competing financial interests.

Figure 1 | Representative aerodynamic measurements for pitching stability and control effectiveness. Long-tailed taxa (**a**) have a stable equilibrium point at 10-25° (yellow line) and the tail is effective in generating pitching moments at low angles-of attack (pale yellow box). In short-tailed taxa (**b**), the equilibrium point at 0-5° is unstable (red line) and the tail control effectiveness is reduced. One example (*Rhamphorynchus*) drawn from pterosaurs illustrates similar possibilities in a phylogenetically distant taxon.

Figure 2 | Evolution of pitch stability and control effectiveness within the Avialae. Pitching stability is plotted in red hues, indicating stable (pale), marginally stable (medium), and unstable (solid). Control effectiveness of the tail in generating pitching moments is plotted in orange hues, indicating large control effectiveness (pale) or reduced control effectiveness (solid). Control effectiveness of symmetric wing protraction/retraction is plotted in yellow hues indicating large (pale) or reduced (solid). Consilience among the three traits indicates that early in the evolution of the Avialae, taxa are stable with a large degree of pitch control from the tail; later taxa are unstable, and control has migrated from the now reduced tail, to the wings, which become larger and develop skeletal features that would enhance control and the production of left-right and fore-aft asymmetries.

Figure 3 | Evolution of roll stability and control effectiveness in the Avialaes. Characters shown are stability at low angle of attack (mostly unstable due to symmetry; *Zhongornis* and *Sapeornis* marginal); stability at high angles of attack (all stable); and control effectiveness of asymmetric wing tucking in roll (always effective). As animals developed the ability to fly at reduced body angles of attack, more active control of roll would have been necessary, at first perhaps using inertial modes of the tail, but subsequently augmented with the forewings.

Figure 4 | Evolution of yaw stability and control effectiveness in the Avialaes. At high angles of attack (**a**), taxa are mostly marginally stable as might be expected from symmetry. Asymmetric pronation and supination of the wings are always effective in generating yaw at high angles of attack. At reduced angles of attack (**b**), by contrast, long-tailed taxa are stable and can control yaw with the tail. As tails reduce in size, taxa become unstable in yaw at low angles of attack and lose the ability to control yaw with the tail. However, asymmetric movements of the wings are effective in producing yaw throughout the evolution of this clade, and control would thus have shifted from the tail to the forewings paralleling the shifts seen in pitch.

Extended Figure 5 | Fossils used for comparative study. Outgroups (**a**) *Anchiornis*[12] and (**b**) *Microraptor*[11]; Fossil Avialans (**c**) *Archaeopteryx*[10,13], (**d**) *Jeholornis*[26,27], (**e**) *Zhongornis*[28], (**f**) *Sapeornis*[29], (**g**) *Zhongjianiornis*[6] and (**h**) *Confuciusornis*[28.30]; (**i**) extant birds *Alectoris*, *Columba*, *Larus*, and *Buteo*.

Extended Figure 6 | Model construction, testing, and measurement of static stability and control effectiveness. Models were developed in Blender (**a**) from fossils (*Archaeopteryx* shown) and constructed and tested (**b**) using established methods[3]. For simple cases such as a sphere or a weather vane, the relationship between slope and stability (**c**) is observed by plotting pitching moments versus angle-of-attack. Nondimensionalized moment coefficients are used to diagnose/examine stability and control effectiveness of the various taxa (**d**).

Extended Figure 7 | Appendage movements tested to determine control effectiveness. Appendage movements were selected based on those observed to be effective in previous work[3], including (**a**) symmetric wing protraction (e.g. wing sweep); (**b**) tail dorsiflexion; (**c**) tucking of one wing; (**d**) tail lateral flexion; and (**e**) asymmetric wing pronation/supination.

Extended Table 1 | Static stability and control effectiveness in pitch. (**a**) Pitch stability coefficients are shown as mean± s.d., n=15. (**b**) Control effectiveness in pitch using tail dorsiflexion (Extended Figure 7b), shown as mean± s.d., n=5. (**c**) Control effectiveness in pitch using symmetric wing protraction (wing sweep) (Extended Figure 7a), shown as mean± s.d., n=5. Colors indicate characters depicted in Figure 2.

Extended Table 2 | Static stability and control effectiveness in roll. (**a**) Roll stability coefficients are shown as mean± s.d., n=15. (**b**) Control effectiveness in roll using asymmetric wing tucking (Extended Figure 7c), shown as mean± s.d., n=5

Extended Table 3 | Static stability and control effectiveness in yaw. (**a**) Yaw stability coefficients are shown as mean± s.d., n=15. (**b**) Control effectiveness in yaw using tail lateral flexion (Extended Figure 7d), shown as mean± s.d., n=5. (**c**) Control effectiveness in yaw using symmetric wing pronation (Extended Figure 7d), shown as mean± s.d., n=5. (**d**) Control effectiveness in yaw using head lateral flexion for pterosaurs only, shown as mean± s.d., n=5.

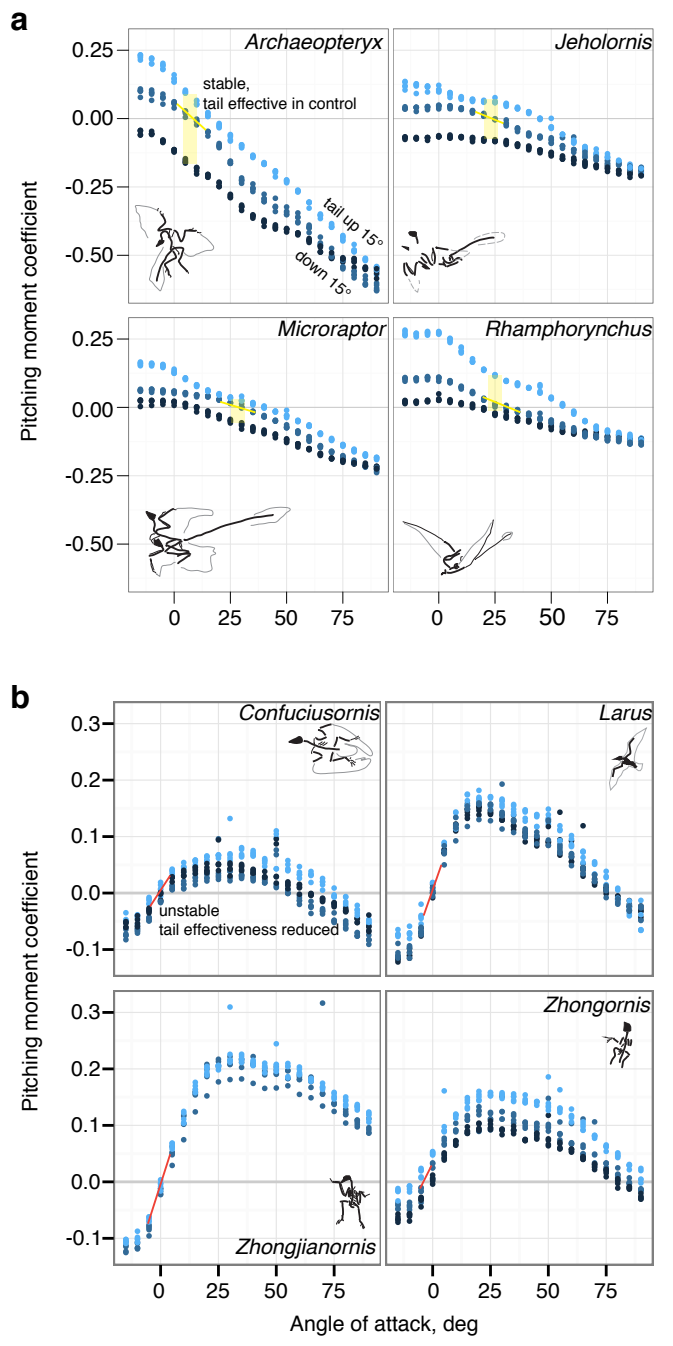
a
Archaeopteryx
stable,
tail effective in control
tail up 15°
down 15°
Jeholornis
Microraptor
Rhamphorynchus
Pitching moment coefficient
0.25
0.00
-0.25
-0.50
0
25
50
75
b
Confuciusornis
unstable
tail effectiveness reduced
Larus
Zhongornis
Zhongjianornis
0.3
0.2
0.1
0.0
-0.1
Pitching moment coefficient
Angle of attack, deg

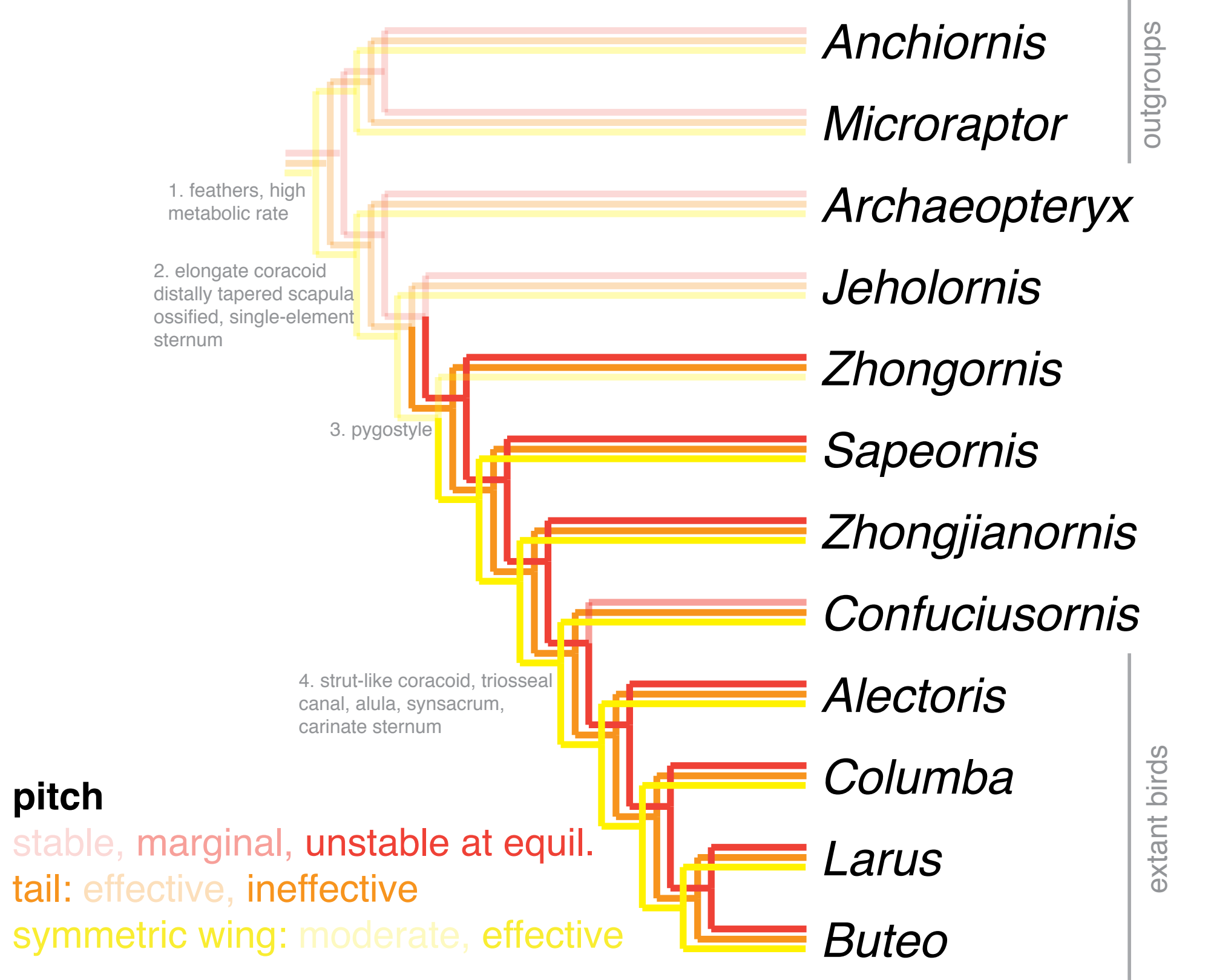
Anchiornis
Microraptor
Archaeopteryx
Jeholornis
Zhongornis
Sapeornis
Zhongjianornis
Confuciusornis
Alectoris
Columba
Larus
Buteo
outgroups
extant birds
1. feathers, high metabolic rate
2. elongate coracoid distally tapered scapula ossified, single-element sternum
3. pygostyle
4. strut-like coracoid, triosseal canal, alula, synsacrum, carinate sternum
pitch
stable, marginal, unstable at equil.
tail: effective, ineffective
symmetric wing: moderate, effective

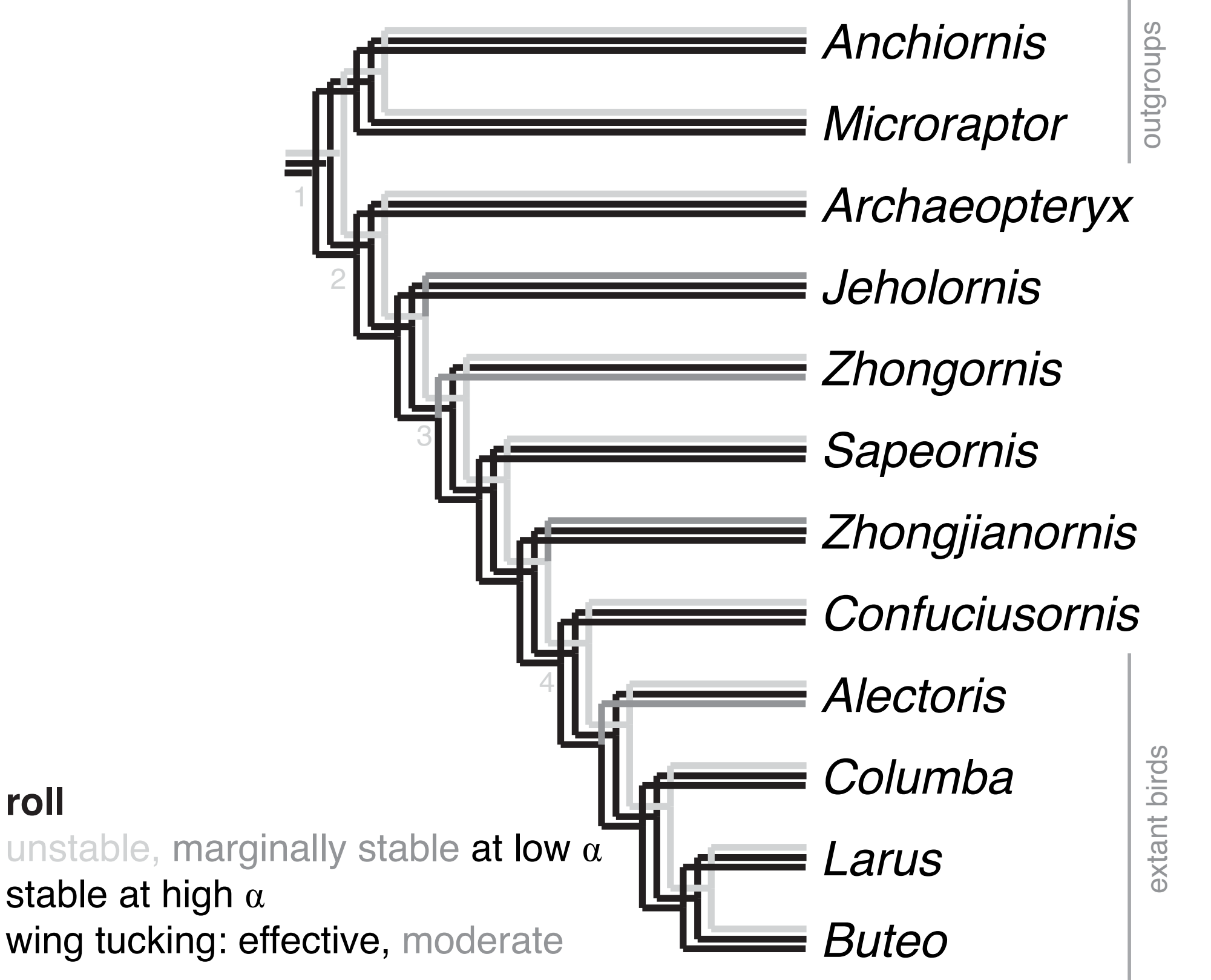
Anchiornis
Microraptor
Archaeopteryx
Jeholornis
Zhongornis
Sapeornis
Zhongjianornis
Confuciusornis
Alectoris
Columba
Larus
Buteo
outgroups
extant birds
1
2
3
4
roll
unstable, marginally stable at low α
stable at high α
wing tucking: effective, moderate

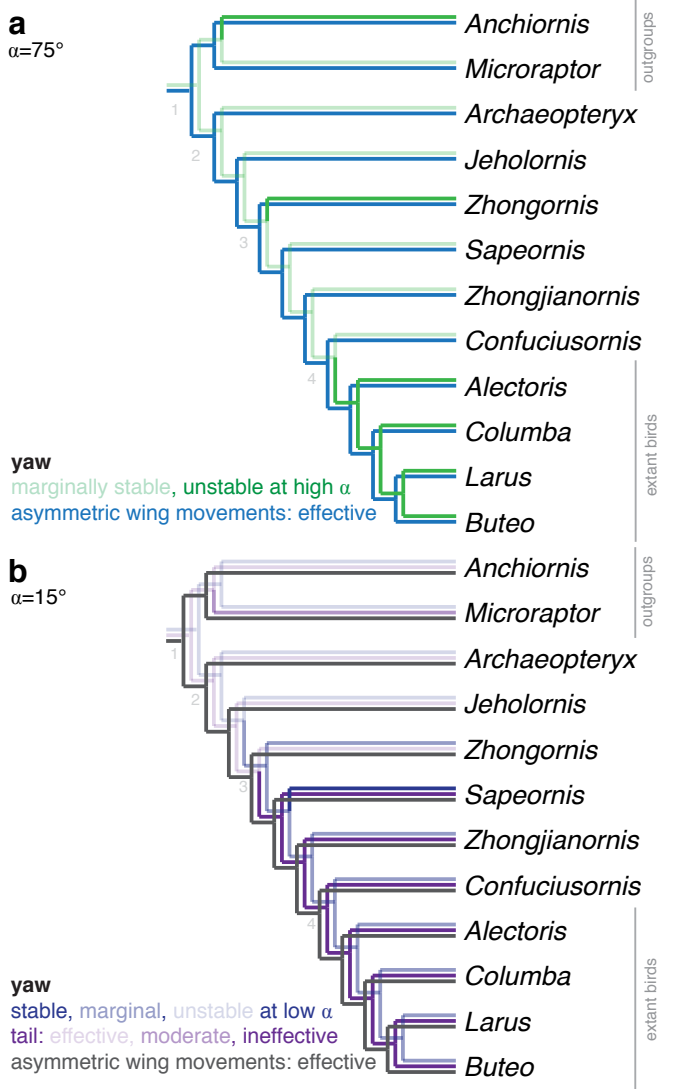
a
α=75°
Anchiornis
Microraptor
Archaeopteryx
Jeholornis
Zhongornis
Sapeornis
Zhongjianornis
Confuciusornis
Alectoris
Columba
Larus
Buteo
outgroups
extant birds
1
2
3
4
yaw
marginally stable, unstable at high α
asymmetric wing movements: effective
b
α=15°
Anchiornis
Microraptor
Archaeopteryx
Jeholornis
Zhongornis
Sapeornis
Zhongjianornis
Confuciusornis
Alectoris
Columba
Larus
Buteo
outgroups
extant birds
1
2
3
4
yaw
stable, marginal, unstable at low α
tail: effective, moderate, ineffective
asymmetric wing movements: effective

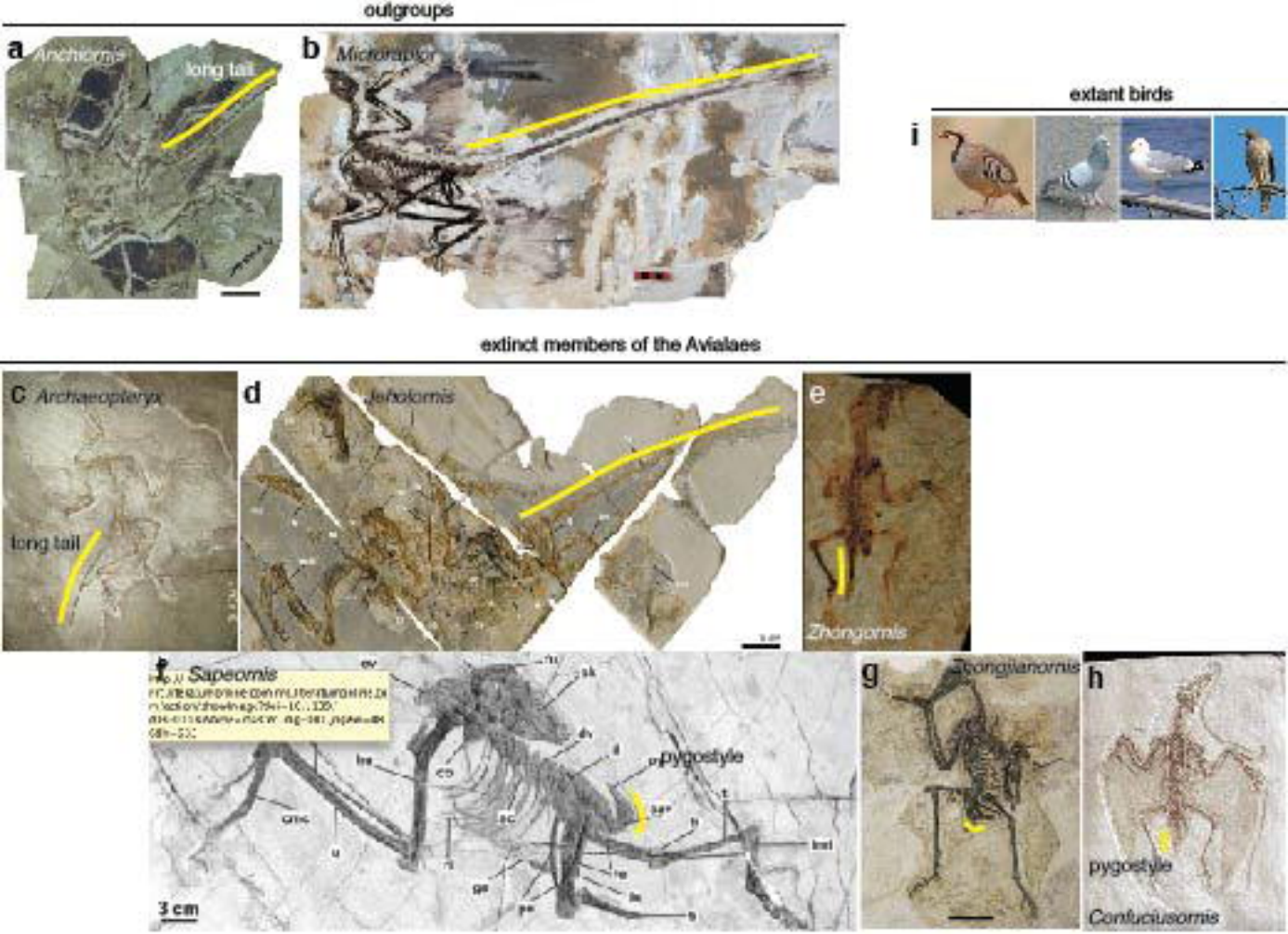
outgroups
a
Anchiornis
long tail
b
Microraptor
extant birds
i
extinct members of the Avialaes
c
Archaeopteryx
long tail
d
Jeholornis
e
Zhongornis
Sapeornis
pygostyle
3 cm
g
Longipteryx
h
pygostyle
Confuciusornis

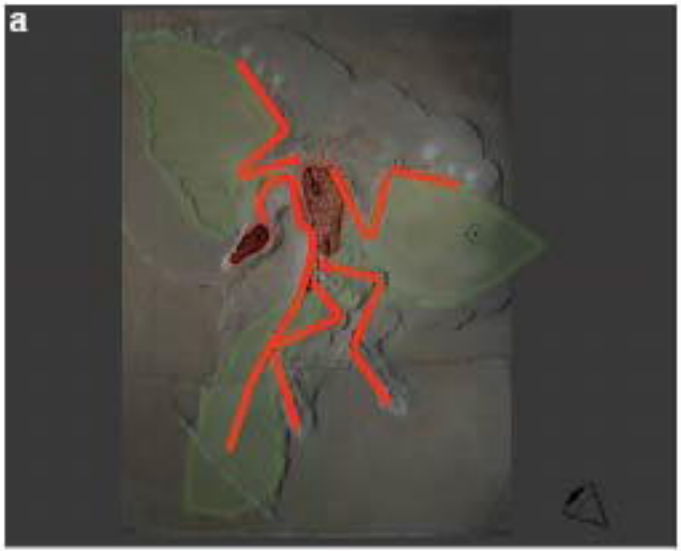
a

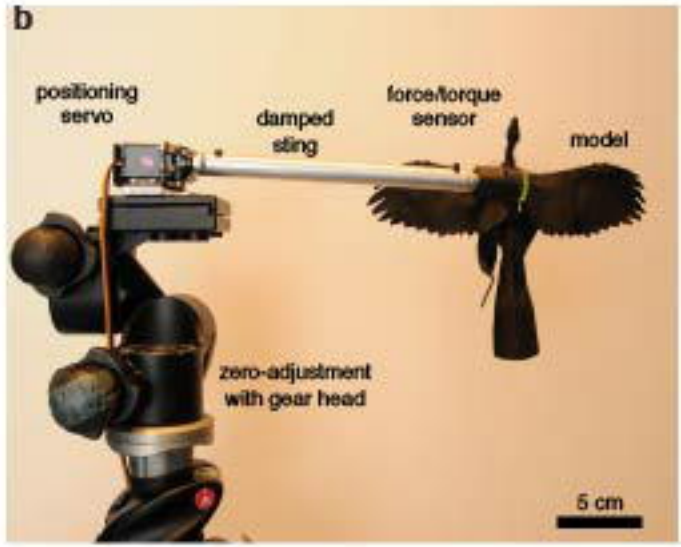
b
positioning servo
damped sting
force/torque sensor
model
zero-adjustment with gear head
5 cm

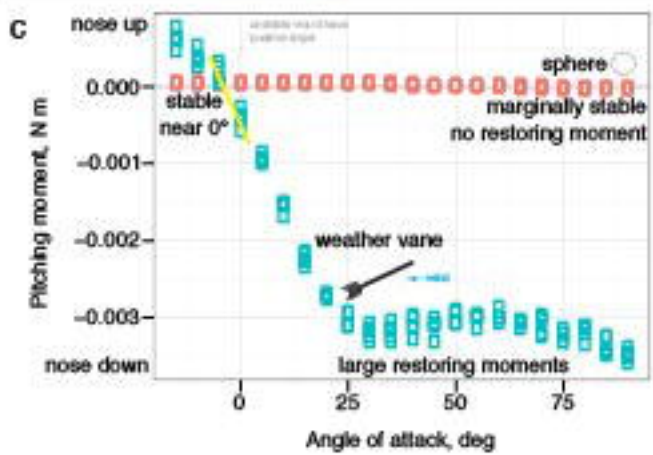
c
nose up
0.000
−0.001
−0.002
−0.003
nose down
Pitching moment, N m
sphere
stable near 0°
marginally stable
no restoring moment
weather vane
large restoring moments
0
25
50
75
Angle of attack, deg

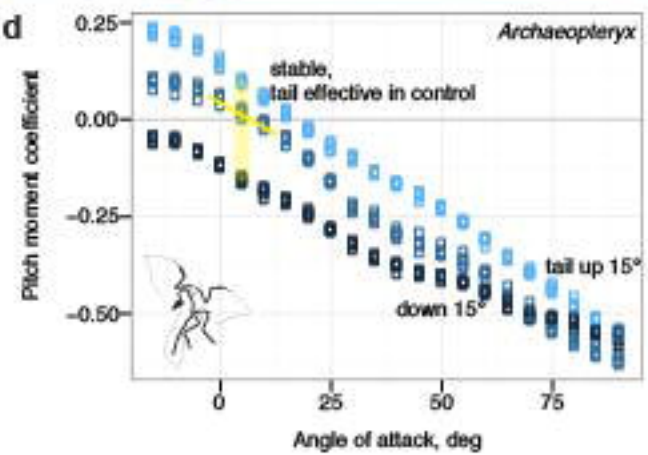
d
0.25
0.00
−0.25
−0.50
Pitch moment coefficient
Archaeopteryx
stable, tail effective in control
tail up 15°
down 15°
0
25
50
75
Angle of attack, deg

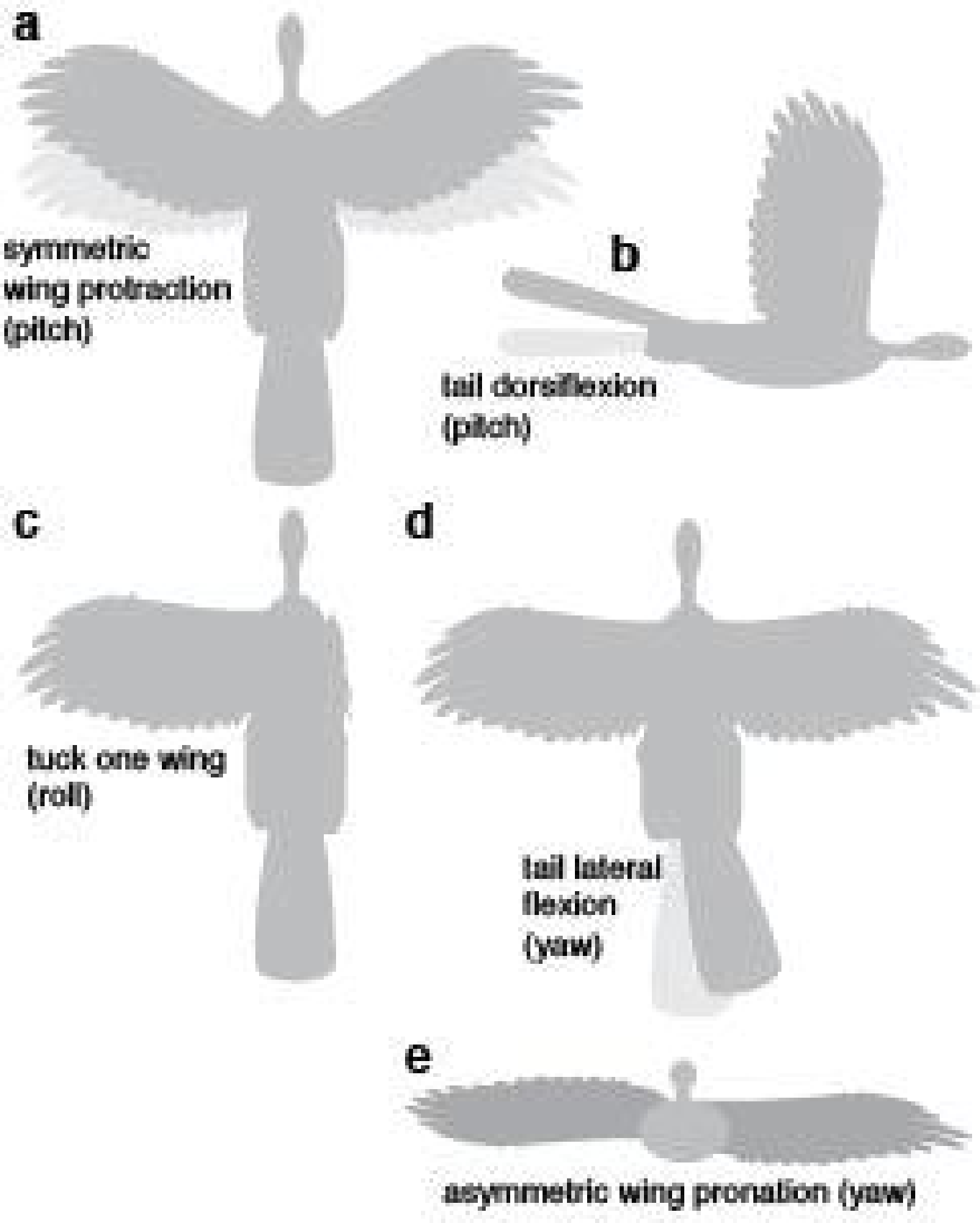
a
symmetric
wing protraction
(pitch)
b
tail dorsiflexion
(pitch)
c
buck one wing
(roll)
d
tail lateral
flexion
(yaw)
e
asymmetric wing pronation (yaw)

a

	pitch stability, $dC_m/d\alpha$			equilibrium point	
	α=0°	α=15°	α=75°	α°	equilibrium $dC_m/d\alpha$
Anchiornis	-0.005±0.013	-0.067±0.012	-0.13±0.03	29±2	**-0.170±0.028**
Archaeopteryx	-0.134±0.013	-0.221±0.020	-0.18±0.03	9±2	**-0.190±0.012**
Confuciusornis	0.142±0.009	0.039±0.020	-0.06±0.02	0±2	**-0.030±0.073**
Jeholornis	0.011±0.018	-0.108 ±0.010	-0.10±0.02	25±1	**-0.120±0.044**
Microraptor	-0.039±0.006	-0.071±0.009	-0.17±0.02	20±2	**-0.070±0.029**
Sapeornis	0.109±0.010	0.007±0.011	-0.11±0.02	5±2	**-0.100±0.052**
Zhongjianornis	0.305±0.036	0.195±0.027	-0.15±0.16	5±1	**0.180±0.078**
Zhongornis	0.237±0.021	0.084±0.017	-0.11±0.09	0±2	**0.060±0.089**
Alectoris	0.206±0.006	0.090±0.020	-0.37±0.16	0±1	**0.120±0.013**
Buteo	0.187±0.010	-0.042±0.009	-0.13±0.02	0±3	**-0.140±0.030**
Columba	0.046±0.014	-0.047±0.017	-0.18±0.16	0±6	**-0.050±0.088**
Larus	0.352±0.028	0.092±0.015	-0.10±0.02	0±1	**0.150±0.049**
Onychonycteris	-0.011±0.011	-0.112±0.005	-0.12±0.02	10±2	-0.110±0.033
Pteropus	-0.118±0.014	-0.055±0.008	-0.10±0.02	0±2	-0.080±0.015
Pteranodon	0.054±0.023	0.004±0.018	-0.07±0.04	5±3	-0.050±0.029
Pterodactylus	-0.020±0.020	-0.050±0.009	-0.05±0.03	0±4	-0.040±0.009
Rhamphorynchus	-0.062±0.013	-0.192±0.024	-0.05±0.01	15±1	-0.180±0.044
Sphere	-0.037±0.023	-0.020±0.022	-0.03±0.01		-0.050±0.006
Weather vane	-0.333±0.040	-0.347±0.020	-0.03±0.04	0±2	-0.210±0.055

b

	control effectiveness, $dC_m/d\delta$ for tail dorsiflexion*		
	α=0°	α=15°	α=75°
Anchiornis	0.168±0.002	**0.191±0.006**	0.0467±0.0120
Archaeopteryx	0.219±0.007	**0.190±0.010**	0.0649±0.240
Confuciusornis	0.011±0.003	**0.013±0.003**	0.0178±0.0050
Jeholornis	0.268±0.019	**0.223±0.001**	0.0678±0.0050
Microraptor	0.174±0.023	**0.125±0.002**	0.0891±0.0140
Sapeornis	0.054±0.001	**0.064±0.005**	0.0817±0.0060
Zhongjianornis	0.023±0.004	**0.019±0.004**	0.0124±0.0260
Zhongornis	0.049±0.006	**0.048±0.002**	0.0455±0.0030
Alectoris	0.011±0.004	**0.012±0.005**	0.0443±0.0070
Buteo	0.018±0.003	**0.033±0.012**	0.0491±0.0060
Columba	0.044±0.004	**0.050±0.003**	0.0085±0.0020
Larus	0.014±0.008	**0.016±0.003**	0.0137±0.0080
Onychonycteris	0.029±0.004	0.032±0.002	0.004±0.004
Pteropus	0.053±0.009	0.026±0.003	0.026±0.002
Pteranodon	0.016±0.005	0.015±0.002	0.0158±0.0030
Pterodactylus	0.015±0.002	0.025±0.004	0.0388±0.0050
Rhamphorynchus	0.347±0.016	0.245±0.032	0.0288±0.0100

c

	control effectiveness, $dC_m/d\delta$ for symmetric wing protraction†		
	α=0°	α=15°	α=75°
Anchiornis	0.00±0.02	**0.050±0.020**	0.070±0.004
Archaeopteryx	-0.00253±0.016	**0.060±0.018**	0.128±0.0036
Confuciusornis	0.00640±0.034	**0.117±0.023**	0.229±0.0015
Jeholornis	0.04239±0.009	**0.072±0.006**	0.088±0.002
Microraptor	0.01784±0.008	**0.037±0.003**	0.051±0.0036
Sapeornis	0.02174±0.038	**0.173±0.039**	0.329±0.001
Zhongjianornis	0.02522±0.027	**0.119±0.023**	0.221±0.0006
Zhongornis	0.02976±0.012	**0.069±0.010**	0.100±0.0006
Alectoris	-0.00095±0.017	**0.124±0.020**	0.119±0.0017
Buteo	0.04297±0.034	**0.142±0.021**	0.213±0.0013
Columba	0.07612±0.027	**0.151±0.013**	0.168±0.0002
Larus	-0.00706±0.030	**0.110±0.032**	0.231±0.0012
Onychonycteris	0.03101±0.030	0.152±0.031	0.235±0.0025
Pteropus	-0.00490±0.041	0.131±0.030	0.230±0.0023
Pteranodon	0.16728±0.050	0.315±0.033	0.480±0.0014
Pterodactylus	0.00492±0.026	0.088±0.018	0.141±0.0023
Rhamphorynchus	0.01197±0.025	0.045±0.020	0.175±0.0007

* movement depicted in Extended Figure 7b
† movement depicted in Extended Figure 7a

a

	roll stability, $dC_m/d\phi$	
	α=15°	α=75°
Anchiornis		
Archaeopteryx	0.009±0.060	-0.200±0.019
Confuciusornis	-0.020±0.020	-0.200±0.09
Jeholornis	0.073±0.030	-0.400±0.025
Microraptor	0.132±0.030	-0.300±0.019
Sapeornis	0.043±0.040	-0.300±0.026
Zhongjianornis	0.030±0.020	-0.200±0.012
Zhongornis	0.017±0.040	-0.100±0.080
Alectoris	0.009±0.060	-0.100±0.016
Buteo	0.028±0.050	-0.400±0.022
Columba	-0.030±0.050	-0.300±0.014
Larus	-0.009±0.020	-0.400±0.028
Onychonycteris		-1.000±0.044
Pteropus	-0.027±0.050	-0.700±0.064
Pteranodon	0.011±0.020	-0.200±0.014
Pterodactylus	-0.002±0.060	-0.300±0.016
Rhamphorynchus	-0.0969±0.030	-0.400±0.021
Sphere	0 (exact)	0 (exact)

b

	control effectiveness, $dC_m/d\delta$ for asymmetric wing tucking*	
	α=15°	α=75°
Anchiornis		
Archaeopteryx	0.090±0.005	0.200±0.018
Confuciusornis	0.050±0.002	0.100±0.012
Jeholornis	0.080±0.004	0.120±0.024
Microraptor	0.050±0.007	0.170±0.021
Sapeornis	0.080±0.002	0.130±0.016
Zhongjianornis	0.050±0.001	0.140±0.015
Zhongornis	0.030±0.001	0.050±0.007
Alectoris	0.060±0.002	0.080±0.007
Buteo	0.170±0.012	0.240±0.055
Columba	0.180±0.007	0.180±0.027
Larus	0.150±0.004	0.200±0.038
Onychonycteris	0.810±0.036	0.880±0.100
Pteropus	0.680±0.020	0.830±0.088
Pteranodon	0.070±0.002	0.100±0.010
Pterodactylus	0.100±0.003	0.110±0.027
Rhamphorynchus	0.160±0.007	0.210±0.030

* movement depicted in Extended Figure 7c

a

	yaw stability, $dC_m/d\psi$	
	α=15°	α=75°
Anchiornis	**-0.097±0.003**	**0.006±0.006**
Archaeopteryx	**-0.070±0.004**	**0.010±0.004**
Confuciusornis	**-0.026±0.002**	**0.004±0.002**
Jeholornis	**-0.091±0.003**	**0.002±0.001**
Microraptor	**-0.100±0.016**	**0.039±0.010**
Sapeornis	**0.002±0.003**	**0.005±0.0004**
Zhongjianornis	**0.021±0.003**	**0.008±0.002**
Zhongornis	**0.014±0.002**	**0.00±0.81**
Alectoris	**0.022±0.001**	**0.001±0.002**
Buteo	**0.027±0.006**	**-0.002±0.004**
Columba	**0.048±0.002**	**0.003±0.002**
Larus	**0.017±0.004**	**0.002±0.002**
Onychonycteris	0.025±0.008	-0.040±0.007
Pteropus	0.040±0.025	-0.160±0.005
Pteranodon	0.026±0.002	0.002±0.0004
Pterodactylus	-0.002±0.001	0.002±0.001
Rhamphorynchus	-0.052±0.004	-0.034±0.004

b

	control effectiveness, $dC_m/d\delta$ for lateral tail flexion*	
	α=15°	α=75°
Anchiornis	**0.240±0.070**	0.067±0.013
Archaeopteryx	**0.220±0.070**	0.066±0.004
Confuciusornis	**0.002±0.001**	-0.004±0.001
Jeholornis		-0.027±0.007
Microraptor	**0.520±0.083**	-0.076±0.010
Sapeornis		
Zhongjianornis	**-0.001±0.002**	-0.007±0.001
Zhongornis	**0.007±0.002**	-0.011±0.001
Alectoris	**0.019±0.012**	-0.050±0.001
Buteo	**-0.007±0.003**	-0.029±0.003
Columba	**0.005±0.002**	-0.022±0.001
Larus		-0.012±0.002
Onychonycteris	-0.011±0.005	-0.012±0.003
Pteropus (no tail)		
Pteranodon (no tail)		
Pterodactylus (no tail)		
Rhamphorynchus	0.170±0.008	0.128±0.002

c

	control effectiveness, $dC_m/d\delta$ for asymmetric wing supination†	
	α=15°	α=75°
Anchiornis	**0.199±0.020**	**0.330±0.004**
Archaeopteryx	**0.420±0.015**	**0.383±0.016**
Confuciusornis	**0.206±0.025**	**0.184±0.007**
Jeholornis		
Microraptor	**0.259±0.013**	**0.373±0.008**
Sapeornis		
Zhongjianornis	**0.296±0.015**	**0.262±0.015**
Zhongornis	**0.115±0.006**	**0.113±0.002**
Alectoris	**0.081±0.013**	**0.093±0.004**
Buteo	**0.565±0.060**	**0.431±0.025**
Columba	**0.455±0.042**	**0.204±0.003**
Larus		
Onychonycteris	0.870±0.093	0.627±0.049
Pteropus (no tail)		
Pteranodon (no tail)	0.271±0.013	0.234±0.004
Pterodactylus (no tail)	0.196±0.014	0.139±0.013
Rhamphorynchus	0.279±0.027	0.319±0.024

d

	control effectiveness, $dC_m/d\delta$ for lateral head flexion*	
	α=15°	α=75°
Pteranodon	0.120±0.002	-0.003±0.0005
Pterodactylus	0.190±0.003	0.002±0.001
Rhamphorynchus	-0.033±0.009	

* movement depicted in Extended Figure 7d
† movement depicted in Extended Figure 7e